Fur -Dam regulatory interplay at an internal promoter of the enteroaggregative Escherichia coli Type VI secretion sci1 gene cluster

Yannick R Brunet, Christophe S Bernard, E. Cascales

Fur – Dam Regulatory Interplay at An Internal Promoter of the Enteroaggregative *Escherichia coli* Type VI Secretion *sci1* Gene Cluster.

Yannick R. Brunet[†], Christophe S. Bernard[¶], and Eric Cascales*

Running head: Regulation of the EAEC *sci1* T6SS gene cluster.

Laboratoire d'Ingénierie des Systèmes Macromoléculaires (LISM), Institut de Microbiologie de la Méditerranée (IMM), CNRS – Aix-Marseille Université UMR7255, 31 chemin Joseph Aiguier, 13402 Marseille Cedex 20, France.

* To whom correspondence should be addressed. E-mail: cascales@imm.cnrs.fr

[†] Current address: Department of Microbiology and Immunobiology, Harvard Medical School, 77 Avenue Louis Pasteur, Boston, MA, 02115 USA.

[¶] Current address: Laboratoire de Chimie Bactérienne (LCB), Institut de Microbiologie de la Méditerranée (IMM), CNRS – Aix-Marseille Université UMR7283, 31 chemin Joseph Aiguier, 13402 Marseille Cedex 20, France.

Characters count (including spaces): 48,000
Tables: 0
Figures: 7
Supplemental material: 2 Figures

ABSTRACT

The type VI secretion system (T6SS) is a weapon widespread in Gram-negative bacteria that delivers effectors into target cells. The T6SS is a highly versatile machine as it can target both eukaryotic and prokaryotic cells, and it has been proposed that T6SS are adapted to the specific needs of each bacterium. The expression of T6SS gene clusters and the activation of the secretion apparatus are therefore tightly controlled. In enteroaggregative *Escherichia coli* (EAEC), the *sci1* T6SS gene cluster is subjected to a complex regulation involving both the ferric uptake regulator Fur and Dam-dependent DNA methylation. In this study, an additional, internal, promoter was identified within the *sci1* gene cluster using +1 transcriptional mapping. Further analyses demonstrated that this internal promoter is controlled by a mechanism strictly identical to that of the main promoter. The Fur binding box overlaps with the -10 transcriptional element and a Dam methylation site, GATC-32. Hence, the expression of the distal *sci1* genes is repressed and the GATC-32 site is protected from methylation in iron-rich conditions. The Fur-dependent protection of GATC-32 was confirmed by *in vitro* methylation assay. In addition, the methylation of GATC-32 negatively impacts Fur binding. The expression of the *sci1* internal promoter is therefore controlled by iron availability through Fur regulation whereas Dam-dependent methylation maintains a stable ON expression in iron-limited conditions.

IMPORTANCE

Bacteria use weapons to deliver effectors into target cells. One of these weapons, the type VI secretion system (T6SS), assembles a contractile tail acting as a spring to propel a toxin-loaded needle. Its expression and activation therefore need to be tightly regulated. Here we identified an internal promoter within the *sci1* T6SS gene cluster in enteroaggregative *E. coli*. We then show that this internal promoter is controlled by Fur and Dam-dependent methylation. We further demonstrate that Fur and Dam compete at the -10 transcriptional element to finely tune the expression of T6SS genes. We propose that this elegant regulatory mechanism allows the optimum production of the T6SS in conditions where enteroaggregative *E. coli* may encounter competing species.

INTRODUCTION

The fate of microbial communities is governed by communication, cooperation and competition mechanisms between microorganisms (1-9). Bacteria therefore developed an arsenal of signalling, sensing and antagonistic activities. To eliminate competitors, bacteria evolved distinct mechanisms: release of antibiotics or bacteriocins in the extracellular medium, as well as delivery of toxins directly into the target cell (10-12). One of the delivery apparatuses, the type VI secretion system (T6SS), transports effectors into competing bacteria using a mechanism similar to that used by contractile injection systems such as bacteriophages and R-pyocins (13-19). This secretion apparatus is constituted of a ~ 600-nm long cytoplasmic needle-like structure composed of an inner tube tipped by a spike complex that is used to penetrate the membrane of the target cell (12, 14, 19). The inner tube is wrapped by an outer sheath that is assembled under an extended metastable conformation (20, 21). The tail tube/sheath complex is built on a baseplate that is anchored to the cell envelope by a membrane complex (22-29). Tail tube/sheath assembly, which can be visualised *in vivo* by fluorescence microscopy, is completed in a few tens of seconds (30-32). Contraction of the sheath powers the propulsion of the inner tube to deliver effectors into the target cell (15, 17, 31, 33-35). Effectors are usually charged within the inner tube lumen or loaded onto the spike complex via direct interactions with the VgrG/PAAR spike or via adaptor proteins (36-45).

The T6SS is a very efficient mechanism and hence is an important player in the regulation of the microbiota (7, 46). Bacteria equipped with this apparatus colonize more efficiently the environmental niche and hence have a better access to the resources (47-51). Most of the T6SS gene clusters are not constitutively expressed and T6SS-dependent antagonistic activities are usually deployed once cells experience stress or nutrient starvation conditions (52-57). T6SS gene clusters are therefore subjected to a tight regulation that

89 involves sensing of the environmental conditions (52, 53, 55). Most known regulatory
90 mechanisms are hijacked by T6SSs for their regulation: transcriptional activators and
91 repressors, alternate sigma factors, histone-like proteins, two-component transduction
92 cascades, or quorum-sensing systems (52, 53). In addition, a number of T6SSs are post-
93 translationally activated by a threonine phosphorylation pathway in response to cell damages
94 or envelope stresses (58).

95 Enteroaggregative *Escherichia coli* (EAEC) is equipped with two functional T6SSs,
96 named Sci1 (T6SS-1 subfamily) and Sci2 (T6SS-3 subfamily) (59, 60). These two T6SSs
97 confer antagonistic activities but are not expressed in the same conditions, suggesting that
98 T6SS-mediated anti-bacterial activities are required in two conditions that EAEC may
99 encounter during its life cycle (31, 44). The *sci2* gene cluster is expressed during infection
100 conditions and is activated in laboratory conditions when cells are grown in a synthetic
101 medium mimicking the macrophage environment (59). This *sci2* gene cluster is under the
102 control of the AraC-like AggR transcriptional regulator (59), which also modulates the
103 expression of most biofilm determinants (59, 61), suggesting that the Sci2 T6SS is required
104 for eliminating competing bacteria during aggregation, a phenomena that occurs during host
105 colonization. By contrast, the *sci1* gene cluster is expressed in minimal synthetic media, and
106 has been shown to be under the dual control of the ferric uptake repressor (Fur) and Dam-
107 dependent methylation (62).

108 To gain further information on the *sci1* gene cluster organization, we defined its
109 operon structure. RT-PCR experiments showed that all genes are contiguous suggesting that
110 all the genes are present on a single mRNA or on several overlapping mRNAs. Using +1
111 transcriptional mapping, we confirmed the existence of a promoter region upstream the first
112 gene of the cluster but revealed an additional promoter located upstream the *EC042_4532*

gene, within the *EC042_4531* gene coding sequence. We further identified a Fur-binding sequence overlapping with the -10 transcriptional box and demonstrated that Fur binds with high affinity and prevents RNA polymerase access to the promoter. Sequence analyses showed that this Fur box overlaps with a GATC Dam methylation site, GATC-32. *In vivo*, we showed that Fur prevents methylation of the GATC-32 site when cells grew in iron-replete conditions. *In vitro* competition experiments confirmed that Fur prevents GATC-32 methylation. In addition, we observed that Dam-dependent methylation of GATC-32 decreases the affinity of Fur for its Fur box. Taken together, our results demonstrate that a second functional, internal promoter controls the expression of T6SS *sci1* genes and that this promoter is under a regulatory mechanism identical to the main promoter.

RESULTS AND DISCUSSION

Operon structure of the *sci1* T6SS gene cluster. We previously reported that the promoter located upstream the *tssB* gene, *i.e.*, the first gene of the EAEC *sci1* T6SS gene cluster, contains operator sequences for the Ferric uptake regulator, Fur, as well as an overrepresentation of GATC motifs which are targets of the DNA adenine methylase Dam. Using *in vivo* and *in vitro* Fur binding and methylation assays, we delineated the contribution of these two regulators on the expression of the *tssB* gene (62). However, whether additional or internal promoters exist, and whether the entire gene cluster is subjected to this regulatory control remained undetermined. The EAEC *sci1* gene cluster is a ~ 26-kb DNA fragment present on the *pheU* pathogenicity island (Fig. 1A; 59). Prediction of the open reading frames (ORF) within this fragment shows that it encodes 21 gene products including the 14 T6SS core components, a toxin-immunity pair, and accessory genes or of unknown function (genes *tssB* to *tssE*, see Fig. 1A). With the exception of a large intergenic sequence (162-pb between

the *hcp* and the *clpV* genes), most of the start and stop codons of contiguous genes overlap or are separated by few (< 8) nucleotides (see Fig S1 in supplemental material). This genomic organization suggests that translational coupling must occur, and that the expression of these genes must be coordinated. To test whether the *sci1* gene cluster is organized as a single genetic unit, or constituted of several operons, we performed reverse-transcriptase - polymerase chain reactions (RT-PCR) using oligonucleotides designed for the amplification of each gene junction (numbered 1-21; see Fig. 1A). RT-PCR experiments were performed on purified total RNAs extracted from cells grown in Sci1-inducing medium (SIM) (Fig. 1B; upper panel). As controls, RT-PCR reactions were performed on purified genome DNA (Fig. 1B, middle panel), as well as on the total RNA preparation but in absence of reverse transcriptase to test for DNA contamination (Fig. 1B, lower panel). As shown on Fig. 1B, RT-PCR products with expected sized were obtained for each gene junction of the *sci1* gene cluster from DNA or cDNA, but not from RNA (Fig. 1B, lanes 2-21), suggesting that the 21 genes are co-transcribed. As expected, the *Ec042_4523* ORF, upstream the first gene of the *sci1* cluster, and in the reverse orientation compared to the *tss* genes, is not co-transcribed with *tssB* (Fig. 1B, lane 1). These results suggest that all the *sci1* genes are present on a unique polycistronic mRNA, or that overlapping mRNAs are expressed from internal promoters.

An additional promoter is located upstream *EC042_4532*. To identify potential internal promoter(s), we used an *in silico* approach. Analysis of the T6SS *sci1* gene cluster using the BProm algorithm (Softberry; available at http://linux1.softberry.com/berry.phtml) suggested the existence of an additional promoter with a σ^{70} -10 element upstream the *EC042_4532* gene. To test whether an internal promoter is present upstream of *Ec042_4532*, we used 5'-RACE assay. mRNAs were extracted from EAEC cells grown in SIM and subjected to primer extension. The putative *tssB* promoter, was also included in this assay.

The results showed that transcription of the *tssB* mRNA starts at the base A, located 73 bases upstream the ATG start codon of *tssB* (colored red in Fig. 2A). The *tssB* transcription starts are therefore compatible with the putative -10 and -35 transcription boxes identified through *in silico* analyses in our previous study (62) (Fig. 2A). A transcriptional start was also detected upstream the *EC042_4532* gene, suggesting the existence of an active internal promoter. The position of the identified transcriptional start (base G located 117 bases upstream the ATG of *EC042_4532*, colored red in Fig. 2B) is compatible with the location of the -10 element predicted by the BProm algorithm (Fig. 2B).

***In silico* sequence analyses of the *EC042_4532* promoter region identify Fur and Dam sites overlapping with the -10 element.** Interestingly, the BProm computer program also identified a putative Fur binding box in the *EC042_4532* promoter region (hereafter called Fur-32). This putative operator sequence overlaps with the -10 of transcription (Fig. 2B and 2C). This situation is reminiscent of the main promoter, which is repressed by the Fur protein in an iron-dependent manner (62). One of the Fur boxes contained in the *tssB* promoter contains a Dam-dependent methylation site (Fig. 2A), and we previously reported that Fur and Dam compete at this specific site to fine tune the expression of the *sci1* gene cluster (62). Strikingly, a GATC motif is also found within the putative Fur-32 box of the *EC042_4532* promoter (Fig. 2C, hereafter called GATC-32). Taken together, the *in silico* sequence analyses raised the question whether the internal promoter is under a similar regulatory mechanism as the *tssB* main promoter.

The P_{4532}-*lacZ* translational fusion is responsive to iron limitation and Fur. To test whether the expression of the internal promoter is regulated by Fur, we engineered a low copy plasmid-borne translational fusion of a 570-bp fragment comprising the *EC042_4532* promoter (from -450 to +120 relative to the transcriptional +1, called hereafter P_{4532}) to *lacZ*.

186 The *β*-galactosidase activity of this P_{4532}-*lacZ* translational fusion was monitored in the
187 EAEC *lacZ* strain or its *fur* isogenic mutant, in presence or absence of the iron chelator 2,2'-
188 di-pyridyl (dip). Figure 3 shows that the expression of the P_{4532} translational fusion increased
189 ~ 6-fold in the WT strain upon treatment with the iron chelator. Compared to the WT strain in
190 absence of iron chelator, the activity of the translational fusion increased ~ 13-fold in the *fur*
191 isogenic background. Treatment of the *fur* mutant strain with 2,2'-dipyridyl had no additional
192 effect on the activity of the P_{4532}-*lacZ* translational reporter fusion (data not shown). From
193 these activities, we concluded that the expression from the P_{4532} promoter is repressed by the
194 Fur transcriptional regulator in an iron-dependent manner.

195 **Fur binds to the P_{4532} promoter and limits access to the RNA polymerase.** To test
196 whether Fur binds the *EC042_4532* promoter region *in vitro*, the purified *E. coli* Fur protein
197 and the radiolabeled P_{4532} 570-bp fragment were used for electrophoretic mobility shift assays
198 (EMSA). As controls, and as previously published (62), Fur bound to the *sci1* promoter,
199 yielding two bands due to the presence of two Fur boxes, but did not retard the Fur-
200 independent *sci2* promoter (Fig. 4A, lanes 8-10). Fur also shifted the P_{4532} fragment in
201 presence of iron, its co-repressor (Fig. 4A, lanes 1-5; Fig. 4B). This shift was strictly
202 dependent on metal-bound Fur, as no band retardation could be observed when the fragment
203 and the purified regulator were incubated in presence of the metal chelator EDTA (Fig. 4A,
204 lane 6). By contrast, control experiments showed that the σ^{54} enhancer binding protein NtrC
205 did not bind the P_{4532} fragment (Fig. 4A, lane 7). From these data, we conclude that Fur binds
206 to the P_{4532} promoter *in vitro*, likely to the putative Fur-32 box.

207 Fur repression is usually caused by preventing access of the RNA polymerase (RNAP) to the
208 promoter. We hypothesized that such a mechanism might be likely at promoter P_{4532} as the
209 putative Fur-32 box overlaps with the -10 RNAP-binding element (Fig. 2B). We therefore

tested whether σ^{70}-RNAP holoenzyme binds to the P_{4532} promoter and whether Fur influences σ^{70}-RNAP binding. Fig. 4C shows that the σ^{70}-RNAP complex binds to the P_{4532} promoter (Fig. 4C, lanes 1-3) and that pre-incubation of the P_{4532} fragment with Fur prevents binding of the σ^{70}-RNAP, demonstrating that Fur and RNAP compete for binding on P_{4532} (Fig. 4C, lanes 4-6; Fig. 4D).

Dam methylation at the GATC-32 site decreases RNAP binding to the P_{4532} promoter. To gain insight on the contribution of Dam to the regulation of *EC042_4532*, we measured the *β*-galactosidase activity of the P_{4532}-*lacZ* translational fusion in *dam* and *fur-dam* EAEC strains. Deletion of *dam* did not cause a significant variation of the activity of the promoter fusion compared to its parental wild-type strain (Fig. 3). By contrast, the activity of the promoter fusion in the *fur-dam* strain increased ~ 16-fold compared to the wild-type strain, and ~ 1.4-fold compared to the *fur* mutant. These results show that Dam and Fur have additive negative effects on the regulation at the P_{4532} promoter, and that the contribution of Dam is masked in presence of Fur. Based on these results, we hypothesized that GATC-32 methylation affects RNAP binding. A Dam-methylated P_{4532} fragment was subjected to EMSA with the reconstituted σ^{70}-RNAP complex. As shown in Fig. 4C and Fig. 4D, σ^{70}-RNAP binding was diminished on the methylated P_{4532} fragment.

Fur-Dam competition at the P_{4532} promoter. The observation that the Dam effect was masked by Fur *in vivo* raised the idea that, similarly to the P_{sci1} situation, Fur binding to the Fur-32 box prevents Dam-methylation of the GATC-32 site. To test this hypothesis, *in vitro* and *in vivo* assays were conducted.

Fur binding at the P_{4532} *promoter prevents GATC-32 methylation* in vitro. To test the impact of Fur binding on GATC-32 methylation *in vitro*, we added purified Dam methylase to radiolabeled P_{4532} fragments pre-incubated or not with purified Fur protein. The P_{4532}

fragments were then used for enzymatic digestion using enzymes that cleave GATC motifs (Fig S2 in supplemental material). We used the advantage that the GATC-32 site is part of a larger palindromic sequence, TgatcA, which is the target for BclI, a restriction enzyme that is sensitive to Dam methylation (Fig S2 in supplemental material). In addition to GATC-32, the P_{4532} fragment contains a GATC site at position 149 ($GATC^{149}$) that does not overlap with a Fur box (Fig S2 in supplemental material). Fig. 5A shows that, as expected, incubation with the Dam methylase caused methylation of the GATC sites as P_{4532} is cleaved in three fragments when incubated with DpnI, an enzyme that specifically recognizes methylated GATC motifs. In agreement with this result, P_{4532} was resistant to MboI and BclI, two enzymes that are sensitive to GATC adenine methylation (Fig. 5A, middle panel). When the P_{4532} fragment was pre-incubated with Fur, only the $GATC^{149}$ site was digested by DpnI. By contrast, only the GATC-32 site was digested by MboI or BclI (Fig. 5A, right panel). These experiments demonstrate that in presence of Fur, $GATC^{149}$ is methylated whereas GATC-32 is not, suggesting that Fur protects GATC-32 methylation by steric occlusion.

Fur binding at the P_{4532} *promoter prevents GATC-32 methylation* in vivo. The methylation status of the P_{4532} GATC sites was then tested *in vivo*. The pGE573 plasmid bearing the P_{4532}-*lacZ* fusion was extracted from various genetic backgrounds, the *Eco*R1-*Bam*H1 fragment comprising the P_{4532} promoter was purified and the methylation state of GATC-32 was assessed by restriction. In the WT strain grown in LB medium, the MboI and BclI enzymes cleaved GATC-32 (Fig. 5B, left panel), revealing that this site is un-methylated. The absence of methylation is likely due to the presence of Fur bound to the Fur box overlapping with GATC-32 as GATC-32 was methylated in the *fur* isogenic background (Fig. 5B, right panel) or when WT cells were grown in presence of the 2,2'-dipyridyl iron chelator (Fig. 5B, third panel from left).

Taken together, the results of the *in vitro* and *in vivo* Dam methylation assays demonstrate that Fur binding on the Fur-32 box prevents access of the Dam methylase to the GATC-32 site in iron rich conditions. By contrast, Fur repression is relieved in iron limiting conditions and the GATC-32 site is then methylated.

GATC-32 Dam methylation decreases the affinity of Fur to the P_{4532} *promoter.* The observation that the GATC-32 site is methylated once Fur repression is relieved raised the question whether methylation of the GATC-32 motif interferes with Fur binding. We therefore performed mobility shift assays with Fur using the P_{4532} fragment, methylated by Dam *in vitro*. Fig. 6 shows that methylation of GATC-32 caused a significant decrease of affinity of Fur for the P_{4532} promoter.

Concluding remarks

In this study, we report the presence of an internal promoter within the *sci1* T6SS gene cluster of enteroaggregative *E. coli*. The presence of internal promoters that serve as transcriptional re-starts or that are necessary to ensure proper stoichiometric production is common in large gene clusters. It has been well documented for gene clusters encoding amino-acid synthesis pathways such as histidine, tryptophan, threonine, or branched chain amino-acids (63-67). More recently, an internal promoter within the gene cluster encoding the ESX-3 type VII secretion system has been identified in *Mycobacterium smegmatis* (68). Here, we show that this internal promoter, P_{4532}, is under the control of a regulatory mechanism similar to that controlling the main promoter (Fig. 7): expression from the P_{4532} promoter is repressed by the Fur protein, that binds to a Fur box overlapping with the -10 transcriptional element. In addition, a GATC site, GATC-32, which is a target of the Dam methylase,

281 overlaps with the Fur binding box. In iron rich conditions, Fur binding to the promoter
282 prevents methylation of this motif. However, during iron starvation, Fur removal allows
283 methylation of the GATC-32 site and the methylation decreases the affinity of Fur for its
284 binding box. Therefore Fur controls the switch between ON and OFF expression, whereas
285 Dam methylation stabilizes the ON phase (Fig. 7). This mechanism is therefore similar to that
286 previously reported for the *sci1* main promoter (62). However, differences can be noticed.
287 First, the level of methylation and the activity of the Dam methylase might be slightly
288 different on the main and the internal promoters, as the sequences flanking the GATC motifs
289 have different AT content. Indeed, sequences flanking Dam sites have been previously shown
290 to modulate the catalytic activity or the processivity of Dam (69). Second, a ~13-fold
291 derepression of the internal promoter is observed in absence of Fur, while a >25-fold
292 derepression was observed for the main promoter (62). These results are in agreement with
293 the lower consensus of the Fur-32 box compared to the Fur box overlapping with the -10 of
294 the main promoter (Fig. 2C), and with the potential cooperativity of the two Fur-binding
295 boxes at the main promoter (62).

296 The role of the Dam methylase in transcriptional gene regulation is well documented.
297 In addition to its role in mismatch repair and replication initiation, Dam is involved in
298 epigenetic control of the expression of many genes including genes encoding type III
299 secretion systems, adhesins, fimbriae, or involved in lipopolysaccharide modifications (for
300 reviews, see 70-72). GATC sites can be found in intergenic regions, and in some cases these
301 sites overlap with transcriptional elements such as the -10 (73). Hence Dam-dependent
302 methylation may directly impact transcription. However, in most cases, GATC sites found in
303 promoter regions do not overlap with transcriptional elements, but rather with regulator
304 binding boxes. In these cases, the methylation status may control binding of the regulator, and
305 reciprocally, regulator binding may prevent methylation of certain GATC sites. Several

studies have reported competition between Dam-dependent methylation and regulator fixation, such as the OxyR repressor at the *agn43* promoter, or the Lrp repressor at the *pap* operon promoter (74-76). In general, competition between methylation and regulator binding results in the transition between OFF and ON expression phases (72).

In conclusion, the *sci1* gene cluster is subjected to Fur/Dam regulation, and a transcriptional re-start occurs after the eighth gene of the operon. Further experiments will be necessary to define whether this re-start is necessary because transcription of the mRNA from the initial promoter stops before the last gene, or because the distal part of the operon requires additional copies of mRNA for proper stoichiometry.

MATERIAL AND METHODS

Bacterial strains, plasmids, medium, and growth conditions. *E. coli* K-12 strain DH5a was used for all cloning procedures. The EAEC strains used in this study are all derivatives of 17-2 and have been previously described (62). The plasmid-borne P_{4532}-*lacZ* fusion was engineered by ligating a blunt-end 570-bp fragment encompassing the 4532 promoter (corresponding to bases –450 to +120, respective to the *EC042_4532* transcriptional start site [nucleotides 4892656-4893121], amplified from EAEC 17-2 chromosomal DNA using oligonucleotides 5'-CGCACCATGATCGTCTCTGTATCGC and 5'-CTGAAACGAACTGCTCATGGCTCTCTC) into the *Sma*I-linearized pGE573, a vector that carries a promoter-less *lacZ* gene (77). In this construct, the *lacZ* gene is under the control of the P_{4532} promoter. Proper insertion, orientation and sequence of the fragment into the pGE-P_{4532} plasmid were verified by restriction, PCR and DNA sequencing (MWG). *E. coli* cells were routinely grown in Luria Broth (LB) or Sci1-inducing medium (SIM; M9 minimal medium supplemented with glycerol 0.25 %, vitamin B1 200 µg.mL^{-1}, casaminoacids 40 µg.mL^{-1}, $MgCl_2$ 2 mM, $CaCl_2$ 0.1 mM, and LB (10% v/v); 62) supplemented with antibiotics when necessary (kanamycin 50 µg.mL^{-1}, ampicillin 100 µg.mL^{-1} for K-12 or 200 µg.mL^{-1} for EAEC).

RNA purification. EAEC total RNAs have been extracted using the PureYield^{TM} RNA midiprep system (Promega) from 8×10^9 cells grown in SIM and harvested in exponential growth phase (optical density at λ=600nm [OD_{600}] ~ 0.8). RNAs were eluted with 1 mL of water, cleared with DNaseI

(Ambion™), and precipitated overnight at – 80°C by ammonium sulfate/ethanol procedures. The RNA pellet was washed and resuspended in 45 µL of nuclease-free water. RNA quality and integrity were tested on agarose gel, and by the absorbance ratio at λ=260/280 nm. The absence of DNA contamination was further tested by PCR using 35 cycles of amplification. Quantifications gave an average RNA concentration of 70 $\mu g.mL^{-1}$. Total RNAs were then subjected to RT-PCR (Access RT-PCR, Promega) or transcriptional +1 mapping (5'RACE, Invitrogen).

Reverse transcription – PCR. The Reverse transcription (RT) and PCR have been performed with the one-tube procedure, using the Access RT-PCR system (Promega), with 200 ng of total RNA and oligonucleotides allowing amplification of 550-750-bp regions overlapping the two contiguous genes (see Fig. 1A; primer sequences available upon request), following the supplier's guidelines. Briefly, both reverse transcriptase and Tfl Taq polymerase were added in each tube. The reverse transcription was carried out for 45 min at 45°C, and, after inactivation of the reverse transcriptase at 94°C for 5 min, a 30-cycle PCR was performed (denaturation at 94°C for 30 sec; annealing at 55°C for 40 sec.; and amplification at 68°C for 50 sec.). As negative controls to test for DNA contamination, RT-PCR were also performed in absence of Reverse Transcriptase. As positive controls, the regions overlapping the two contiguous genes have been amplified from 30 ng of genomic DNA.

5'-RACE assay. Total RNAs (80 $\mu g.mL^{-1}$) were subjected to transcriptional +1 mapping using the 5'RACE system (Invitrogen).

***β*-galactosidase assays.** *β*-Galactosidase activity was measured by the method of Miller (78) on whole cells harvested at OD_{600} of 0.8. Reported values represent the average of technical triplicates from three independent biological cultures, and standard deviation are shown on the graphs.

Protein purification. The Fur and NtrC proteins have been purified as described previously (62, 79). The σ^{70}-saturated RNAP holoenzyme has been purchased from USB Corp. The Dam methylase and restriction enzymes have been obtained from New England Biolabs and have been used as recommended by the manufacturer.

Electrophoretic Mobility gel Shift Assay (EMSA) and Dam methylation assays. DNA radiolabeling, EMSA, Fur/RNAP competition EMSA, and *in vivo* and *in vitro* Dam methylation assays have been performed as previously described (62).

Authors contribution

YRB and EC conceived the study and designed the experiments. YRB performed all in vivo and in vitro experiments, with the help of CSB for RNA analyses. YRB and EC analyzed the data. EC wrote the manuscript.

Acknowledgements

We thank Emmanuelle Bouveret and Mireille Ansaldi for sharing strains, plasmids and protocols, Laure Journet and the members of the Cascales, Lloubès, Bouveret and Sturgis research groups for insightful discussions, and Isabelle Bringer, Annick Brun and Olivier Uderso for technical assistance. This work was supported by grants from the Agence Nationale de la Recherche to E.C. (ANR-10-JCJC-1303-03 and ANR-14-CE14-0006-02). Work in EC laboratory is supported by the CNRS, the Aix-Marseille Université, the Fondation pour la Recherche Médicale (DEQ20180339165), and the Fondation Bettencourt-Schueller. Y.R.B. was a recipient of a doctoral fellowship from the French Ministry of Research.

References

1. West SA, Griffin AS, Gardner A. 2007. Evolutionary explanations for cooperation. Curr Biol 17:661–672.
2. Blango MG, Mulvey MA. 2009. Bacterial landlines: contact-dependent signaling in bacterial populations. Curr Opin Microbiol 12:177–81. https://doi.org/10.1016/j.mib.2009.01.011.
3. Strassmann JE, Gilbert OM, Queller DC. 2011. Kin discrimination and cooperation in microbes. Annu Rev Microbiol 65:349–367. https://doi.org/10.1146/annurev.micro.112408.134109.
4. Cornforth DM, Foster KR. 2013. Competition sensing: the social side of bacterial stress responses. Nat Rev Microbiol 11:285–293. https://doi.org/10.1038/nrmicro2977.
5. Aussel L, Beuzón CR, Cascales E. 2016. Meeting report: adaptation and communication of bacterial pathogens. Virulence 7:481–490. https://doi.org/10.1080/21505594.2016.1152441.
6. Rakoff-Nahoum S, Foster KR, Comstock LE. 2016. The evolution of cooperation within the gut microbiota. Nature 533:255–259. https://doi.org/10.1038/nature17626.
7. Chassaing B, Cascales E. 2018. Antibacterial weapons: targeted destruction in the microbiota. Trends Microbiol 26:329–338. https://doi.org/10.1016/j.tim.2018.01.006.
8. García-Bayona L, Comstock LE. 2018. Bacterial antagonism in host-associated microbial communities. Science 361:eaat2456. https://doi.org/10.1126/science.aat2456.
9. Granato ET, Meiller-Legrand TA, Foster KR. 2019. The evolution and ecology of bacterial warfare. Curr Biol 29:521–537. https://doi.org/10.1016/j.cub.2019.04.024.
10. Cascales E, Buchanan SK, Duché D, Kleanthous C, Lloubès R, Postle K, Riley M, Slatin S, Cavard D. 2007. Colicin biology. Microbiol Mol Biol Rev 71:158–229.
11. Ruhe ZC, Low DA, Hayes CS. 2013. Bacterial contact-dependent growth inhibition. Trends Microbiol 21:230–237. https://doi.org/10.1016/j.tim.2013.02.003.

12. Coulthurst S. 2019. The Type VI secretion system: a versatile bacterial weapon. Microbiology 165:503–515. https://doi.org/10.1099/mic.0.000789.
13. Ho BT, Dong TG, Mekalanos JJ. 2014. A view to a kill: the bacterial type VI secretion system. Cell Host Microbe 15:9–21. https://doi.org/10.1016/j.chom.2013.11.008.
14. Zoued A, Brunet YR, Durand E, Aschtgen MS, Logger L, Douzi B, Journet L, Cambillau C, Cascales E. 2014. Architecture and assembly of the Type VI secretion system. Biochim Biophys Acta 1843:1664–1673. https://doi.org/10.1016/j.bbamcr.2014.03.018.
15. Basler M. 2015. Type VI secretion system: secretion by a contractile nanomachine. Philos Trans R Soc Lond B Biol Sci 370:20150021. https://doi.org/10.1098/rstb.2015.0021.
16. Cascales E. 2017. Microbiology: and Amoebophilus invented the machine gun! Curr Biol 27:1170–1173. https://doi.org/10.1016/j.cub.2017.09.025.
17. Brackmann M, Nazarov S, Wang J, Basler M. 2017. Using force to punch holes: mechanics of contractile nanomachines. Trends Cell Biol 27:623–632. https://doi.org/10.1016/j.tcb.2017.05.003.
18. Taylor NMI, van Raaij MJ, Leiman PG. 2018. Contractile injection systems of bacteriophages and related systems. Mol Microbiol 108:6–15. https://doi.org/10.1111/mmi.13921.
19. Cherrak Y, Flaugnatti N, Durand E, Journet L, Cascales E. 2019. Structure and activity of the Type VI secretion system. Microbiol Spectr 7:0031-2019. https://doi.org/10.1128/microbiolspec.PSIB-0031-2019.
20. Kudryashev M, Wang RY, Brackmann M, Scherer S, Maier T, Baker D, DiMaio F, Stahlberg H, Egelman EH, Basler M. 2015. Structure of the type VI secretion system contractile sheath. Cell 160:952–962. https://doi.org/10.1016/j.cell.2015.01.037.
21. Wang J, Brackmann M, Castaño-Díez D, Kudryashev M, Goldie KN, Maier T, Stahlberg H, Basler M. 2017. Cryo-EM structure of the extended type VI secretion system sheath-tube complex. Nat Microbiol 2:1507–1512. https://doi.org/10.1038/s41564-017-0020-7.
22. Aschtgen MS, Gavioli M, Dessen A, Lloubès R, Cascales E. 2010. The SciZ protein anchors the enteroaggregative Escherichia coli Type VI secretion system to the cell wall. Mol Microbiol 75:886–899. https://doi.org/10.1111/j.1365-2958.2009.07028.x.
23. Zoued A, Durand E, Bebeacua C, Brunet YR, Douzi B, Cambillau C, Cascales E, Journet L. 2013. TssK is a trimeric cytoplasmic protein interacting with components of both phage-like and membrane anchoring complexes of the type VI secretion system. J Biol Chem 288:27031–27041. https://doi.org/10.1074/jbc.M113.499772.
24. English G, Byron O, Cianfanelli FR, Prescott AR, Coulthurst SJ. 2014. Biochemical analysis of TssK, a core component of the bacterial Type VI secretion system, reveals distinct oligomeric states of TssK and identifies a TssK-TssFG subcomplex. Biochem J 461:291–304. https://doi.org/10.1042/BJ20131426.
25. Brunet YR, Zoued A, Boyer F, Douzi B, Cascales E. 2015. The type VI secretion TssEFGK-VgrG phage-like baseplate is recruited to the TssJLM membrane complex via multiple contacts and serves as assembly platform for tail tube/sheath polymerization. PLoS Genet 11:e1005545. https://doi.org/10.1371/journal.pgen.1005545.
26. Durand E, Nguyen VS, Zoued A, Logger L, Péhau-Arnaudet G, Aschtgen MS, Spinelli S, Desmyter A, Bardiaux B, Dujeancourt A, Roussel A, Cambillau C, Cascales E, Fronzes R. 2015. Biogenesis and structure of a type VI secretion membrane core complex. Nature 523:555–560. https://doi.org/10.1038/nature14667.
27. Nguyen VS, Logger L, Spinelli S, Legrand P, Huyen Pham TT, Nhung Trinh TT, Cherrak Y, Zoued A, Desmyter A, Durand E, Roussel A, Kellenberger C, Cascales E, Cambillau C. 2017. Type VI secretion TssK baseplate protein exhibits structural similarity with phage receptor-binding proteins and evolved to bind the membrane complex. Nat Microbiol 2:17103. https://doi.org/10.1038/nmicrobiol.2017.103.
28. Cherrak Y, Rapisarda C, Pellarin R, Bouvier G, Bardiaux B, Allain F, Malosse C, Rey M, Chamot-Rooke J, Cascales E, Fronzes R, Durand E. 2018. Biogenesis and structure of a type VI secretion baseplate. Nat Microbiol 3:1404–1416. https://doi.org/10.1038/s41564-018-0260-1.
29. Rapisarda C, Cherrak Y, Kooger R, Schmidt V, Pellarin R, Logger L, Cascales E, Pilhofer M, Durand E, Fronzes R. 2019. In situ and high-resolution cryo-EM structure of a bacterial type VI

secretion system membrane complex. EMBO J 38:e100886. https://doi.org/10.15252/embj.2018100886.
30. Basler M, Pilhofer M, Henderson GP, Jensen GJ, Mekalanos JJ. 2012. Type VI secretion requires a dynamic contractile phage tail-like structure. Nature 483:182–186. https://doi.org/10.1038/nature10846.
31. Brunet YR, Espinosa L, Harchouni S, Mignot T, Cascales E. 2013. Imaging type VI secretion-mediated bacterial killing. Cell Rep 3:36–41. https://doi.org/10.1016/j.celrep.2012.11.027.
32. Kapitein N, Bönemann G, Pietrosiuk A, Seyffer F, Hausser I, Locker JK, Mogk A. 2013. ClpV recycles VipA/VipB tubules and prevents non-productive tubule formation to ensure efficient type VI protein secretion. Mol Microbiol 87:1013–1028. https://doi.org/10.1111/mmi.12147.
33. Cascales E, Cambillau C. 2012. Structural biology of type VI secretion systems. Philos Trans R Soc Lond B Biol Sci 367:1102–1111. https://doi.org/10.1098/rstb.2011.0209.
34. LeRoux M, De Leon JA, Kuwada NJ, Russell AB, Pinto-Santini D, Hood RD, Agnello DM, Robertson SM, Wiggins PA, Mougous JD. 2012. Quantitative single-cell characterization of bacterial interactions reveals type VI secretion is a double-edged sword. Proc Natl Acad Sci USA 109:19804–19809. https://doi.org/10.1073/pnas.1213963109.
35. Basler M, Ho BT, Mekalanos JJ. 2013. Tit-for-tat: type VI secretion system counterattack during bacterial cell-cell interactions. Cell 152:884–894. https://doi.org/10.1016/j.cell.2013.01.042.
36. Silverman JM, Agnello DM, Zheng H, Andrews BT, Li M, Catalano CE, Gonen T, Mougous JD. 2013. Haemolysin coregulated protein is an exported receptor and chaperone of type VI secretion substrates. Mol Cell 51:584–593. https://doi.org/10.1016/j.molcel.2013.07.025.
37. Shneider MM, Buth SA, Ho BT, Basler M, Mekalanos JJ, Leiman PG. 2013. PAAR-repeat proteins sharpen and diversify the type VI secretion system spike. Nature 500:350–353. https://doi.org/10.1038/nature12453.
38. Durand E, Cambillau C, Cascales E, Journet L. 2014. VgrG, Tae, Tle, and beyond: the versatile arsenal of Type VI secretion effectors. Trends Microbiol 22:498–507. https://doi.org/10.1016/j.tim.2014.06.004.
39. Whitney JC, Beck CM, Goo YA, Russell AB, Harding BN, De Leon JA, Cunningham DA, Tran BQ, Low DA, Goodlett DR, Hayes CS, Mougous JD. 2014. Genetically distinct pathways guide effector export through the type VI secretion system. Mol Microbiol 92:529–542. https://doi.org/10.1111/mmi.12571.
40. Alcoforado Diniz J, Coulthurst SJ. 2015. Intraspecies competition in Serratia marcescens is mediated by Type VI-secreted Rhs effectors and a conserved effector-associated accessory protein. J Bacteriol 197:2350–2360. https://doi.org/10.1128/JB.00199-15.
41. Alcoforado Diniz J, Liu YC, Coulthurst SJ. 2015. Molecular weaponry: diverse effectors delivered by the Type VI secretion system. Cell Microbiol 17:1742–1751. https://doi.org/10.1111/cmi.12532.
42. Unterweger D, Kostiuk B, Ötjengerdes R, Wilton A, Diaz-Satizabal L, Pukatzki S. 2015. Chimeric adaptor proteins translocate diverse type VI secretion system effectors in Vibrio cholerae. EMBO J 34:2198–2210. https://doi.org/10.15252/embj.201591163.
43. Whitney JC, Quentin D, Sawai S, LeRoux M, Harding BN, Ledvina HE, Tran BQ, Robinson H, Goo YA, Goodlett DR, Raunser S, Mougous JD. 2015. An interbacterial NAD(P)(+) glycohydrolase toxin requires elongation factor Tu for delivery to target cells. Cell 163:607–619. https://doi.org/10.1016/j.cell.2015.09.027.
44. Flaugnatti N, Le TT, Canaan S, Aschtgen MS, Nguyen VS, Blangy S, Kellenberger C, Roussel A, Cambillau C, Cascales E, Journet L. 2015. A phospholipase A(1) antibacterial Type VI secretion effector interacts directly with the C-terminal domain of the VgrG spike protein for delivery. Mol Microbiol 99:1099–1118. https://doi.org/10.1111/mmi.13292.
45. Unterweger D, Kostiuk B, Pukatzki S. 2017. Adaptor proteins of Type VI secretion system effectors. Trends Microbiol 25:8–10. https://doi.org/10.1016/j.tim.2016.10.003.
46. Coyne MJ, Comstock LE. 2019. Type VI secretion systems and the gut microbiota. Microbiol Spectr 7:0009-2018. https://doi.org/10.1128/microbiolspec.PSIB-0009-2018.

47. Fu Y, Waldor MK, Mekalanos JJ. 2013. Tn-Seq analysis of Vibrio cholerae intestinal colonization reveals a role for T6SS-mediated antibacterial activity in the host. Cell Host Microbe 14:652–663. https://doi.org/10.1016/j.chom.2013.11.001.
48. Bachmann V, Kostiuk B, Unterweger D, Diaz-Satizabal L, Ogg S, Pukatzki S. 2015. Bile salts modulate the mucin-activated Type VI secretion system of pandemic Vibrio cholerae. PLoS Negl Trop Dis 9:e0004031. https://doi.org/10.1371/journal.pntd.0004031.
49. Wexler AG, Bao Y, Whitney JC, Bobay LM, Xavier JB, Schofield WB, Barry NA, Russell AB, Tran BQ, Goo YA, Goodlett DR, Ochman H, Mougous JD, Goodman AL. 2016. Human symbionts inject and neutralize antibacterial toxins to persist in the gut. Proc Natl Acad Sci USA 113:3639–3644. https://doi.org/10.1073/pnas.1525637113.
50. Sana TG, Flaugnatti N, Lugo KA, Lam LH, Jacobson A, Baylot V, Durand E, Journet L, Cascales E, Monack DM. 2016. Salmonella Typhimurium utilizes a T6SS-mediated antibacterial weapon to establish in the host gut. Proc Natl Acad Sci USA 113:5044–5051. https://doi.org/10.1073/pnas.1608858113.
51. Anderson MC, Vonaesch P, Saffarian A, Marteyn BS, Sansonetti PJ. 2017. Shigella sonnei encodes a functional T6SS used for interbacterial competition and niche occupancy. Cell Host Microbe 21:769–776. https://doi.org/10.1016/j.chom.2017.05.004.
52. Bernard CS, Brunet YR, Gueguen E, Cascales E. 2010. Nooks and crannies in type VI secretion regulation. J Bacteriol 192:3850–3860. https://doi.org/10.1128/JB.00370-10.
53. Leung KY, Siame BA, Snowball H, Mok YK. 2011. Type VI secretion regulation: crosstalk and intracellular communication. Curr Opin Microbiol 14:9–15. https://doi.org/10.1016/j.mib.2010.09.017.
54. Silverman JM, Brunet YR, Cascales E, Mougous JD. 2012. Structure and regulation of the type VI secretion system. Annu Rev Microbiol 66:453–472. https://doi.org/10.1146/annurev-micro-121809-151619.
55. Miyata ST, Bachmann V, Pukatzki S. 2013. Type VI secretion system regulation as a consequence of evolutionary pressure. J Med Microbiol 62:663–676. https://doi.org/10.1099/jmm.0.053983-0.
56. LeRoux M, Kirkpatrick RL, Montauti EI, Tran BQ, Peterson SB, Harding BN, Whitney JC, Russell AB, Traxler B, Goo YA, Goodlett DR, Wiggins PA, Mougous JD. 2015. Kin cell lysis is a danger signal that activates antibacterial pathways of Pseudomonas aeruginosa. Elife 4. https://doi.org/10.7554/eLife.05701.
57. LeRoux M, Peterson SB, Mougous JD. 2015. Bacterial danger sensing. J Mol Biol 427:3744–3753. https://doi.org/10.1016/j.jmb.2015.09.018.
58. Mougous JD, Gifford CA, Ramsdell TL, Mekalanos JJ. 2007. Threonine phosphorylation post-translationally regulates protein secretion in Pseudomonas aeruginosa. Nat Cell Biol 9:797–803.
59. Dudley EG, Thomson NR, Parkhill J, Morin NP, Nataro JP. 2006. Proteomic and microarray characterization of the AggR regulon identifies a pheU pathogenicity island in enteroaggregative Escherichia coli. Mol Microbiol 61:1267–1282.
60. Journet L, Cascales E. 2016. The Type VI secretion system in Escherichia coli and related species. EcoSalPlus 7:1–20. https://doi.org/10.1128/ecosalplus.ESP-0009-2015.
61. Morin N, Santiago AE, Ernst RK, Guillot SJ, Nataro JP. 2013. Characterization of the AggR regulon in enteroaggregative Escherichia coli. Infect Immun 81:122–132. https://doi.org/10.1128/IAI.00676-12.
62. Brunet YR, Bernard CS, Gavioli M, Lloubès R, Cascales E. 2011. An epigenetic switch involving overlapping fur and DNA methylation optimizes expression of a type VI secretion gene cluster. PLoS Genet 7:e1002205. https://doi.org/10.1371/journal.pgen.1002205
63. Grisolia V, Carlomagno MS, Bruni CB. 1982. Cloning and expression of the distal portion of the histidine operon of Escherichia coli K-12. J Bacteriol 151:692–700.
64. Grisolia V, Riccio A, Bruni CB. 1983. Structure and function of the internal promoter (hisBp) of the Escherichia coli K-12 histidine operon. J Bacteriol 155:1288–1296.
65. Jackson EN, Yanofsky C. 1972. Internal promoter of the tryptophan operon of Escherichia coli is located in a structural gene. J Mol Biol 69:307–313.

562 66. Saint Girons I, Margarita D. 1985. Evidence for an internal promoter in the Escherichia coli
563 threonine operon. J Bacteriol 161:461–462.
564 67. Wek RC, Hatfield GW. 1986. Examination of the internal promoter, PE, in the ilvGMEDA
565 operon of E. coli K-12. Nucleic Acids Res 14:2763–2777.
566 68. Maciag A, Piazza A, Riccardi G, Milano A. 2009. Transcriptional analysis of ESAT-6 cluster 3
567 in Mycobacterium smegmatis. BMC Microbiol 9:48. https://doi: 10.1186/1471-2180-9-48.
568 69. Peterson SN, Reich NO. 2006. GATC flanking sequences regulate Dam activity: evidence for
569 how Dam specificity may influence pap expression. J Mol Biol 355:459–472.
570 70. Wion D, Casadesús J. 2006. N6-methyl-adenine: an epigenetic signal for DNA-protein
571 interactions. Nat Rev Microbiol 4:183–192.
572 71. Casadesús J, Low D. 2006. Epigenetic gene regulation in the bacterial world. Microbiol Mol
573 Biol Rev 70:830–56.
574 72. Sánchez-Romero MA, Casadesús J. 2020. The bacterial epigenome. Nat Rev Microbiol 18:7–
575 20. https://doi: 10.1038/s41579-019-0286-2.
576 73. Camacho EM, Serna A, Madrid C, Marqués S, Fernández R, de la Cruz F, Juárez A, Casadesús
577 J. 2005. Regulation of finP transcription by DNA adenine methylation in the virulence plasmid
578 of Salmonella enterica. J Bacteriol 187:5691–5699.
579 74. Haagmans W, van der Woude M. 2000. Phase variation of Ag43 in Escherichia coli: Dam-
580 dependent methylation abrogates OxyR binding and OxyR-mediated repression of transcription.
581 Mol Microbiol 35:877–887.
582 75. Waldron DE, Owen P, Dorman CJ. 2002. Competitive interaction of the OxyR DNA-binding
583 protein and the Dam methylase at the antigen 43 gene regulatory region in Escherichia coli. Mol
584 Microbiol 44:509–520.
585 76. Peterson SN, Reich NO. 2008. Competitive Lrp and Dam assembly at the pap regulatory
586 region: implications for mechanisms of epigenetic regulation. J Mol Biol 383:92–105.
587 https://doi: 10.1016/j.jmb.2008.07.086.
588 77. Eraso JM, Weinstock GM. 1992. Anaerobic control of colicin E1 production. J Bacteriol
589 174:5101–5109.
590 78. Miller, J. 1972. Experiments in Molecular Genetics, p. 352-355. Cold Spring Harbor Laboratory,
591 NY.
592 79. Bernard CS, Brunet YR, Gavioli M, Lloubès R, Cascales E. 2011. Regulation of type VI
593 secretion gene clusters by sigma54 and cognate enhancer binding proteins. J Bacteriol
594 193:2158–2167. https://doi.org/10.1128/JB.00029-11.

595

596 **LEGEND TO FIGURES**

597 **FIG 1** Operon structure of the EAEC *sci1* T6SS gene cluster. (A) Schematic organization of the
598 EAEC *sci1* T6SS gene cluster (*EC042_4524* to *EC042_4545*). Genes encoding T6SS core components
599 are indicated in grey. Accessory genes or of unknown function are represented in white. The
600 fragments corresponding to gene junctions and amplified in the RT-PCR experiments are indicated
601 below (1, 692-bp; 2, 672-bp; 3, 550-bp; 4, 618-pb; 5, 586-bp; 6, 643-bp; 7, 748-bp; 8, 629-bp; 9, 575-
602 bp; 10, 654-bp; 11, 581-bp; 12, 768-bp; 13, 762-bp; 14, 459-bp; 15, 600-bp; 16, 673-bp; 17, 576-bp;
603 18, 720-bp; 19, 552-bp; 20, 591-bp; 21, 678-bp). (B) Operon structure of the EAEC *sci1* T6SS gene
604 cluster. Agarose gel analyses of the indicated gene junctions (numbered 1-22, see panel A) amplified
605 by PCR from cDNA (upper panel), genomic DNA (middle panel; positive control) and total RNA
606 (lower panel, negative control). The presence of PCR fragment in the cDNA gels demonstrates co-

607 transcription of the genes located in 5' and 3' of the amplified region. Molecular weight markers (MW,
608 in kb) are indicated on the left. White dashed lines separate different gels combined to a single image.

609 **FIG 2** Regulatory elements of the *sci1* and *4532* promoters. Nucleotide sequences of the *sci1* (A) and
610 *EC042_4532* (B) promoters highlighting overlaps between the transcriptional elements, Fur binding
611 boxes and Dam methylation motifs. The +1 transcriptional site, identified by 5'-RACE are indicated in
612 bold red letters. GATC Dam methylation sites are indicated in bold blue letters. The -10 elements are
613 indicated in green. The underlined sequences indicate Fur binding boxes (italics) and translational start
614 codons. (C) Sequence alignment of the *fur1* (*sci1* promoter) and *fur-32* (*EC042_4532* promoter) boxes
615 with the *E. coli* Fur box consensus sequence. Identical bases are framed in grey. The -10 elements
616 (green letters) and GATC motifs (bold blue letters) are indicated.

617 **FIG 3** The *4532* promoter is under the control of iron levels, Fur and Dam. *β*-galactosidase activity (in
618 Miller units) of a promoterless *lacZ* fusion (white bars) and of the P_{4532}-*lacZ* reporter fusion (blue bars)
619 at OD_{600}=0.8 in the WT EAEC 17-2 strain, after a 30-min treatment with 2,2'-dipyridyl (+dip; 100 µM)
620 or in the isogenic *fur*, *dam* and *fur-dam* mutants.

621 **FIG 4** Fur binds to the *4532* promoter and prevents access to the RNA polymerase *in vitro*. (A)
622 Electrophoretic mobility shift assay of the *EC042_4532* promoter (P_{4532}) with the indicated
623 concentration of Fur in presence of $FeCl_3$ or in presence of EDTA (lane 6) or using purified NtrC
624 transcriptional activator (lane 7). Controls include Fur shift assays of the Fur-dependent *sci1* promoter
625 (lanes 8 and 9) or of the Fur-independent *sci2* promoter (lane 10). DNA-Fur complexes are indicated
626 by stars. The densitometry analysis of Fur binding on the P_{4532} fragment (represented as free P_{4532}
627 DNA as a function of Fur concentration) is shown in panel (B). (C) Electrophoretic mobility shift
628 assay of the unmethylated (P_{4532}, lanes 1-6) or methylated (me-P_{4532}, lanes 7-9) *EC042_4532* promoter
629 with the indicated concentration of σ^{70}-RNAP (in units) alone (lanes 1-3) or in presence of 20 nM of
630 Fur (lanes 4-6). DNA-Fur and DNA-RNAP complexes are indicated by the star and circle respectively.
631 The densitometry analysis of RNAP binding on the unmethylated (blue curve), methylated (green
632 curve) or Fur-bound unmethylated (red curve) P_{4532} fragment (represented as RNAP-bound DNA as a
633 function of RNAP concentration) is shown in panel (D).

634 **FIG 5** Fur protects GATC-32 from methylation *in vitro* and *in vivo*. (A) A radiolabeled PCR product
635 corresponding to the 570-bp P_{4532} fragment was digested by the restriction enzymes indicated on top.
636 Left panel, untreated PCR product; middle panel, PCR product treated with the Dam methylase; right
637 panel, PCR product incubated with purified Fur (20 nM) prior to Dam methylation. Molecular weight
638 markers (MW, in bp) are indicated on the left. The sizes of the digestion products (in bp) are indicated
639 on the right. See Suppl. Fig. S2 for positions of restriction sites and sizes of expected DNA fragments.
640 (B) The P_{4532} promoters isolated from pGE573 vectors carrying the P_{4532}-*lacZ* fusion purified from the

641 EAEC wild-type strain (WT, left panel) or its isogenic *dam* (second panel from left) or *fur* (right panel)
642 mutant strains, or from the WT strain treated with 2,2'-dipyridyl (third panel from left) were digested
643 by the restriction enzymes indicated on top. Molecular weight markers (MW, in bp) are indicated on
644 the left. The sizes of the digestion products (in bp) are indicated on the right. The white dashed lines in
645 left panel indicate reorganization of the lines from the same gel. See Suppl. Fig. S2 for positions of
646 restriction sites and sizes of expected DNA fragments.

647 **FIG 6** GATC-32 methylation influences Fur binding on P_{4532}. (A) Electrophoretic mobility shift assay
648 of the unmethylated (P_{4532}) or methylated (me-P_{4532}) P_{4532} fragment with the indicated concentration of
649 purified Fur. The densitometry analysis of Fur binding on the unmethylated (blue curve) or methylated
650 (green curve) P_{4532} fragment (represented as free P_{4532} DNA as a function of Fur concentration) is
651 shown in panel (B).

652 **FIG 7** Schematic representation of *sci1* gene cluster regulation. (A) The *sci1* T6SS gene cluster is
653 represented on top with the location of the main (P_{Sci1}) and internal (P_{4532}) promoters. Zoom-in genetic
654 architectures of these promoters are shown at bottom (+1, transcriptional start; -10 and -35
655 transcriptional elements [blue]; Fur binding box [orange]; Dam methylation GATC site [green]). (B)
656 Model of regulation of *sci1* main and internal promoters by Fur and Dam. In iron-replete conditions
657 (left), a Fur dimer (orange hexagons) complexed to iron (black dots) is bound to the Fur box,
658 preventing methylation of the GATC site, and access to the RNA polymerase. Expression from the
659 promoter is repressed (OFF state). In iron-limiting conditions (right), Fur is released from the
660 promoter, allowing GATC methylation by Dam and binding of the RNA polymerase. Expression from
661 the promoter is turned on (ON state).

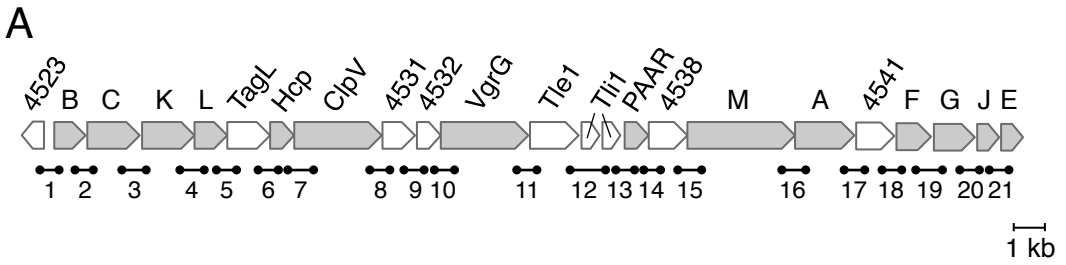

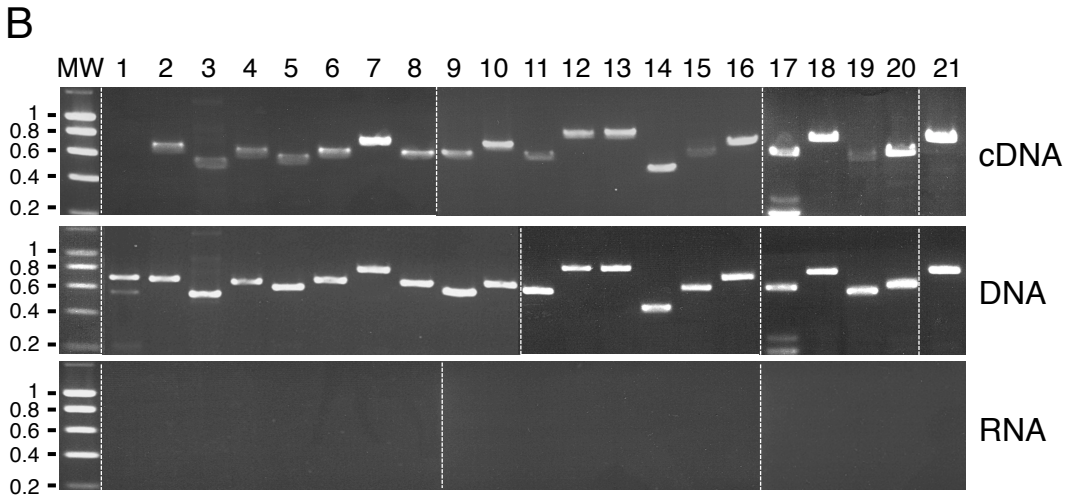

Brunet *et al.*, Figure 1

A P_{sci1}

*CCTGATTATTTGCATTATA*TC**GATC**GATGTATCTG
TTATATTGAGATTTTTCA**GATC**TTCGTCC*TATAAT*
GATC*AAA****A****TTAAA*TCAGTGCACAAGGGGAGGCATC
TGCGGTGATGGAACCCCTGAGATGCAGGTTTCACA
GGAGAGAGCCATG

B P_{4532}

GCGAATATCCCATGGAGCAGCAGGCACAA*ATTATT*
*GCT****GATC****ATTTTA*CTTTGCA**G**GCTGAAGGATACGG
GACATGGTGTGATATGAGAAGGGACGGTGATATCA
CACTGGACGGAAATATGTCTGAGTATGTTATTCGC
AGCCTGTATACCAGCACGTTGCGGGGGTTCCCATG

C

Fur1	TATAAT**GATC**AAAATTAAA
Fur box	GATAATGATAATCATTATC
Fur-32	ATTATTGCT**GATC**ATTTTA

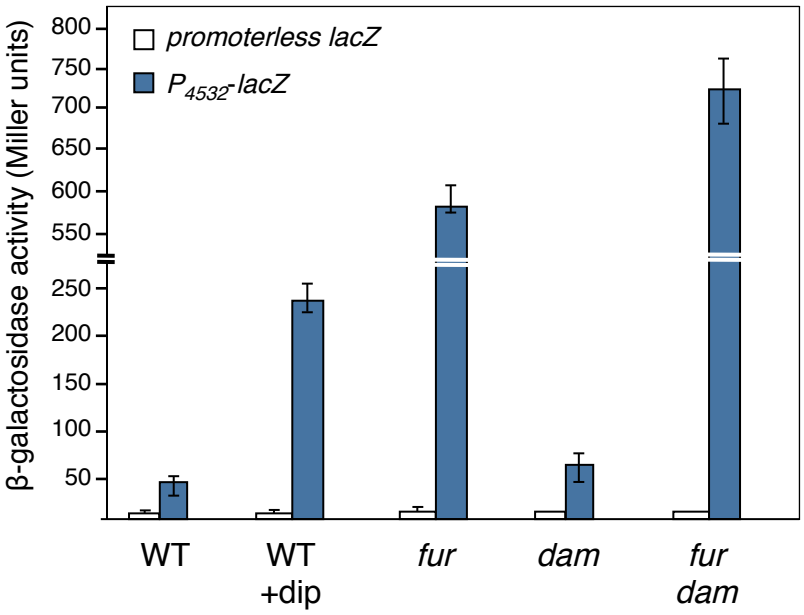

Brunet *et al.*, Figure 3

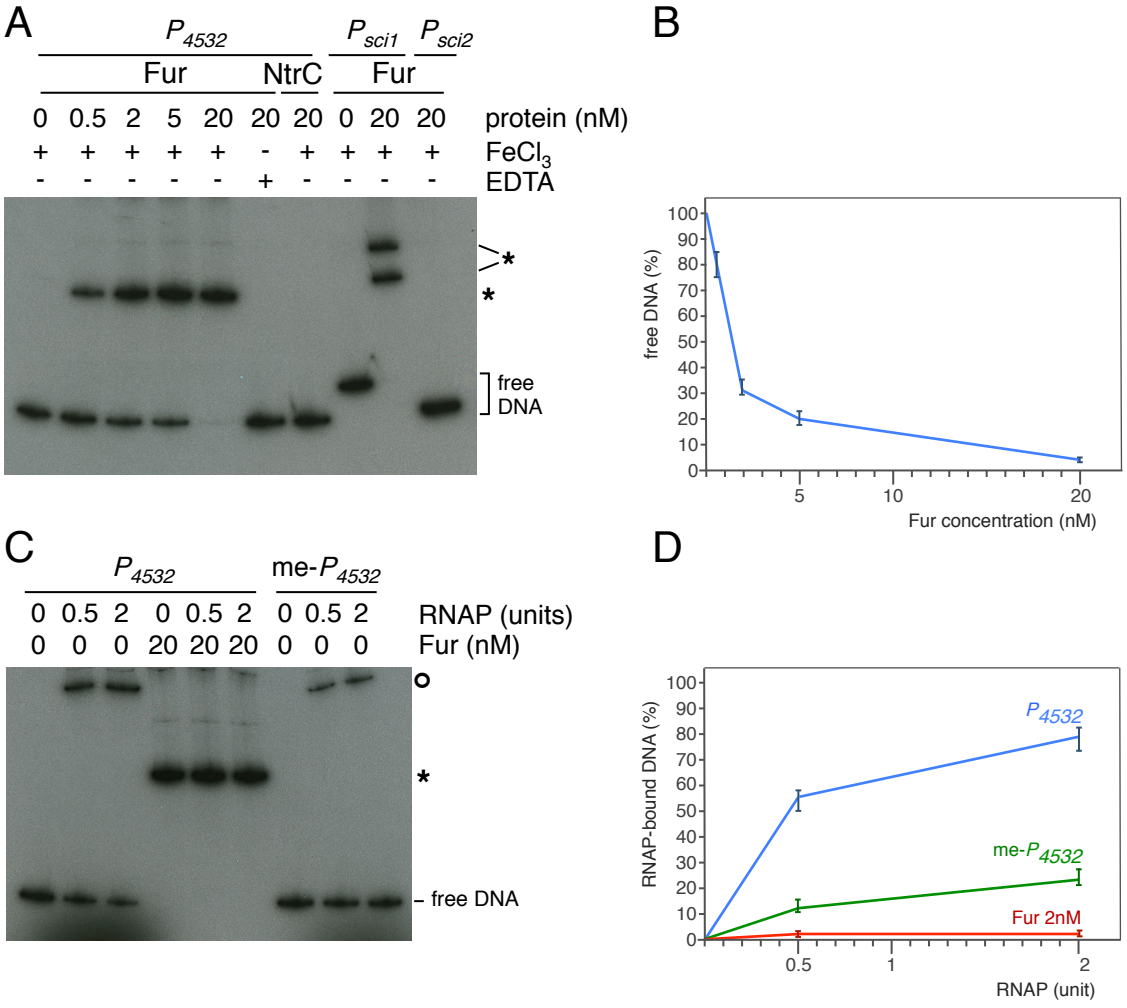

Brunet *et al.*, Figure 4

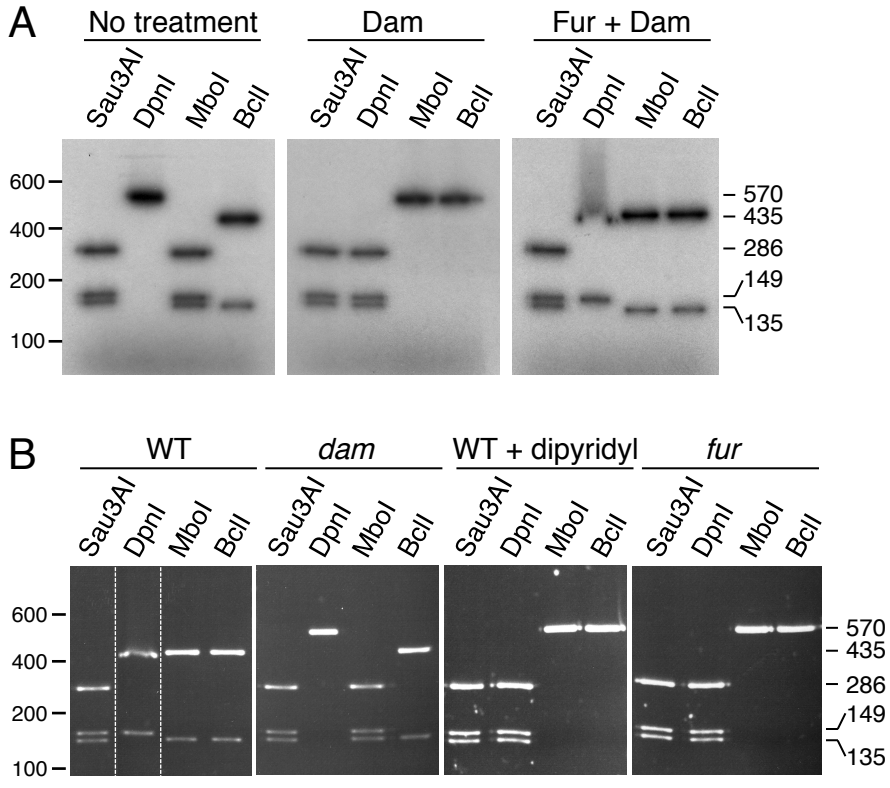

Brunet *et al.*, Figure 5

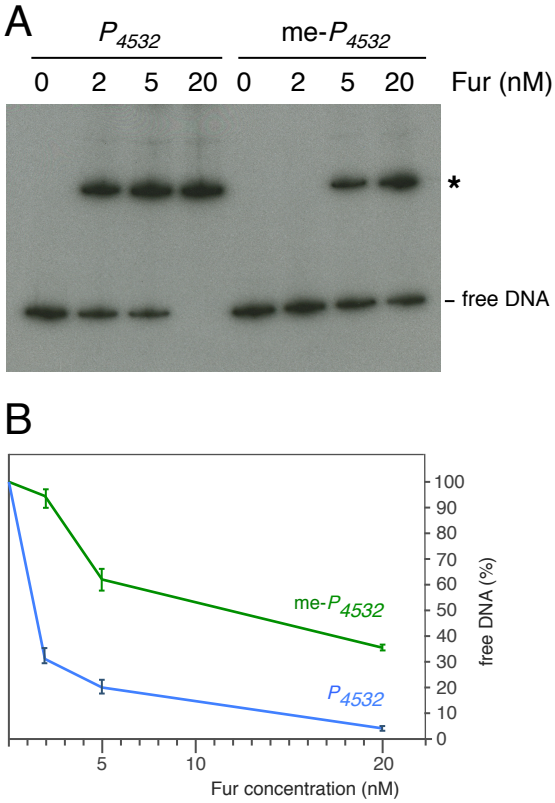

Brunet *et al.*, Figure 6

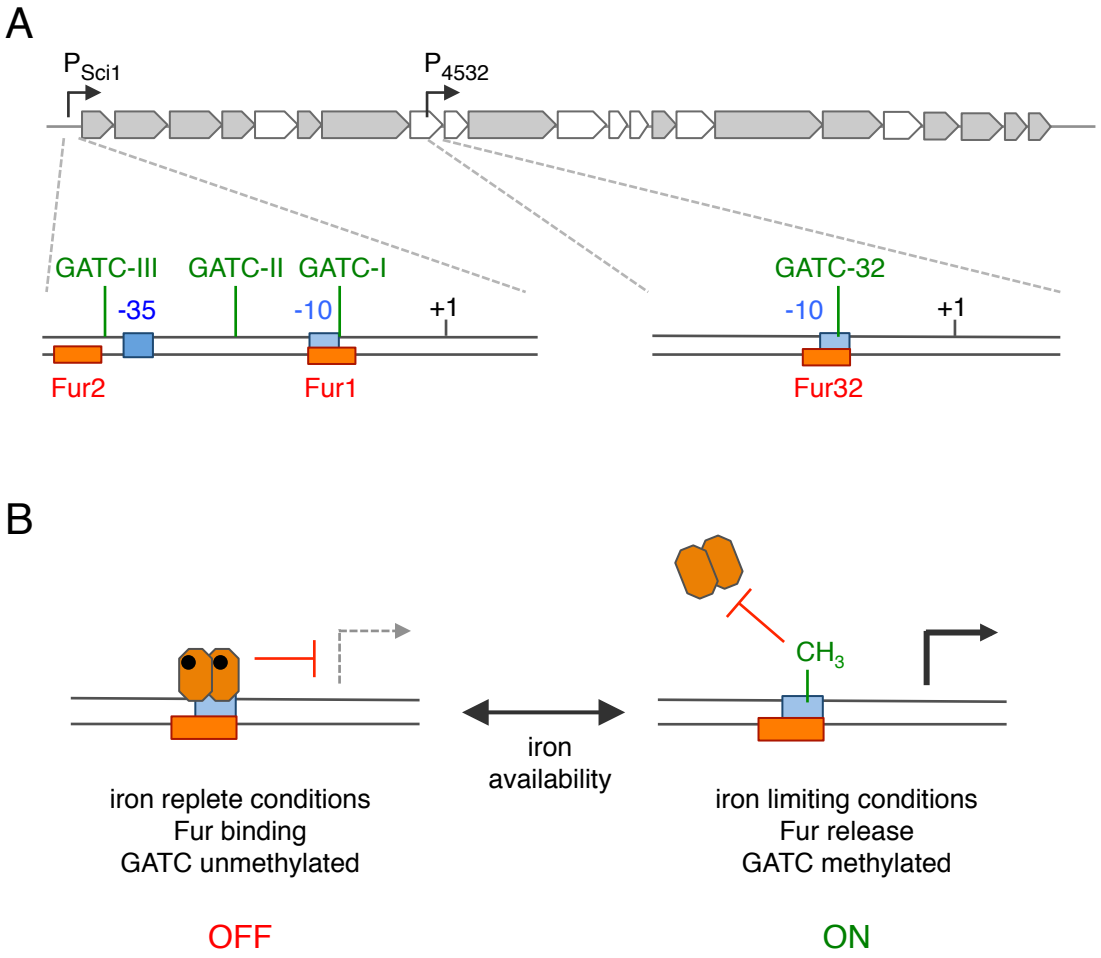

Brunet *et al.*, Figure 7

A

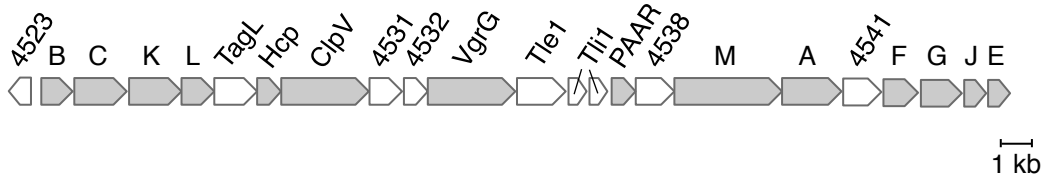

B

tssB-tssC	*tssC-tssK*	*tssK-tssL*	*tssL-tagL*
TGA(N)$_{21}$**atg**	TAA(N)$_{15}$**atg**	c**aTG**Aat -4	TAA(N)$_{2}$**atg**
tagL-hcp	*hcp-clpV*	*clpV-4531*	*4531-4532*
TAA(N)$_{5}$**atg**	TAA(N)$_{159}$**gtg**	tt**aTG**Acc -4	**atg**gTAA -7
4532-vgrG	*vgrG-tle1*	*tle1-tli1*	*tli1b-PAAR*
atgaatctcacTGA -14	ga**aTG**Aca -4	TAA(N)$_{19}$**atg**	TGA(N)$_{31}$**atg**
PAAR-4538	*4538-tssM*	*tssM-tssA*	*tssA-4541*
TAA(N)$_{3}$**atg**	a**atg**aaTAAa -8	gacTG**Atg**gct -1	TGAg**atg**
4541-tssF	*tssF-tssG*	*tssG-tssJ*	*tssJ-tssE*
TGA(N)$_{7}$**atg**	**atg**(N)$_{40}$TAA -46	**atg**(N)$_{14}$TAA -20	TAG(N)$_{2}$**atg**

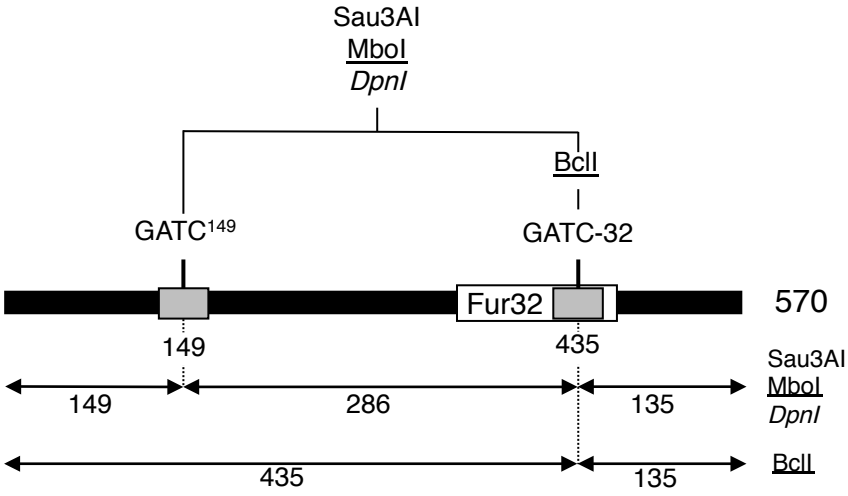

Brunet *et al.*, Figure S2